Study of Fluorescence Quenching Ability of Graphene Oxide with a Layer of Rigid and Tunable Silica Spacer

Xu Wu, Yuqian Xing, Kevin Zeng, Kirby Huber, Julia Xiaojun Zhao*

Department of Chemistry, University of North Dakota, Grand Forks, ND 58202, USA

KEYWORDS. Fluorescence, quenching, graphene oxide, silica nanoparticles

ABSTRACT: The fluorescence quenching property of graphene oxide (GO) has been newly demonstrated and applied for fluorescence imaging and biosensing. In this work, a new nanostructure was designed for effectively studying quenching ability of GO. The key element in this design is the fabrication of a layer of rigid and thickness-adjustable silica spacer for manipulating the distance between the GO and fluorophores. First, a silica core modified with organic dye molecules was prepared, followed by the formation of a silica shell with a tunable thickness. Afterwards, the GO was wrapped around silica nanoparticles based on the electrostatic interaction between negatively charged GO and positively charged silica. The quenching efficiency of GO to different dye molecules was studied at various spacer thicknesses and varying concentrations of GO. Fluorescence lifetime of fluorophores was measured to determine the quenching mechanism. We found that the quenching efficiency of GO was still around 30 % when the distance between dyes and GO was increased to more than 30 nm, which indicated the long-distance quenching ability of GO and confirmed previous theoretical calculation. The quenching mechanisms were proposed schematically based on our experimental results. We expected that the proposed nanostructure could act as a feasible model for studying GO quenching property and shed light on designing GO-based fluorescence sensing systems.

INTRODUCTION

Graphene, a novel two-dimensional carbon nanomaterial, has attracted tremendous research interests due to its excellent optical, electrical, thermal, and surface area properties. 1-3 Using the modified Hummer's method, graphene oxide (GO) can be easily produced and scaled up.4 GO possesses unique optical properties compared to pristine graphene due to the destruction of its sp^2 carbon structure. Band-zero graphene generates adjustable band-gaps in GO, making them suitable for fluorescence imaging and construction of optical devices.5-7 Moreover, oxygen-containing groups, such as carboxyl and hydroxyl groups, provide GO with high aqueous solubility and active sites for further modification.8 In addition to its wellstudied optical property and applications, GO has been recently discovered to be an excellent quencher for fluorophores and quantum dots,9-14 which has been used for the fabrication of fluorescence biosensors. 15-17 For instance, through π - π stacking, a fluorophore-modified single-stranded DNA (ssDNA) can be adsorbed onto the surface of GO, leading to fluorescence quenching. When ssDNA forms a double-stranded DNA (dsDNA) or well-folded structures, the distance between the fluorophore and the GO surface would be increased to restore

the fluorophore's emission. ¹⁸⁻¹⁹ This strategy has been used for sensitive detection of nucleic acids, proteins, small molecules, and metal ions. ²⁰⁻²⁵ These pioneer works have clearly demonstrated the quenching capacity of GO to fluorophores.

The distance between GO and fluorophores is critical in the design of GO' quenching based sensors. Theoretically, the energy transfer rate from a fluorophore to GO is inversely related to the distance between a donor and an acceptor. Theoretical calculation suggests that GO would quench fluorescence at the range of 30 nm.26 In contrast to the traditional fluorescence resonance energy transfer (FRET) process with d⁻⁶ dependency,²⁷ the quenching ability of GOs should be stronger than a traditional quencher. However, an experimental understanding of the GO quenching ability remains elusive due to the ineffective platforms used during the investigation. Recently, Huang et al. 28 and Piao et al. 29 investigated the quenching ability of GO to fluorophores, FAM and Cy3.5. In these works, DNA strands were used as a spacer to separate the fluorophores and GO with variations in the length of DNA strands and the formation of dsDNA strands. The Fröster distance (d₀), which was defined as the distance of 50 % of quenching, was found as 7.5 ± 0.6 nm in Huang's work.²⁸ Piao et al. reported the quenching efficiency of GO increased after 13 DNA bases. The difference among the reported works may imply a folded structure of dsDNAs. Due to the flexibility of DNA strands, even in a dsDNA form, they may tilt at an angle relative to the GO surface. Thus, the distance calculation by counting DNA bases and assuming DNA strands were perpendicular to the surface of GOs could be inaccurate. To overcome the limitation of a DNA spacer, a more rigid spacer is needed for more precise investigations of the quenching ability of GOs to fluorophores.

Herein, we proposed a rigid spacer made of silica layer to fabricate a GO-fluorophore nanostructure. The nanostructure can manipulate an accurate distance between the GO and a fluorophore for a systematic investigation of the quenching ability of GO. The rationale of choosing silica is based on its inert and rigid network structure generated from the hydrolysis and condensation of tetraethylorthosilicate (TEOS). The previous work has demonstrated that a rigid material was a reliable spacer for separating fluorophores and gold nanomaterials in the investigation of metal-enhanced fluorescence. 30-35 In this work the quenching ability of GOs to fluorophores could be delicately measured by coating different thicknesses of silica spacers on the fluorophores. We expected that the proposed nanostructure would be a feasible model for studying GO quenching property and their applications.

EXPERIMENTAL SECTION

Materials and Instruments. Single layer graphene oxide (GO) was purchased from Cheap Tubes Inc., VT. Tris(bipyridine)ruthenium(II) chloride (Rubpy), 1-hexanol (99+ %), tetraethylorthosilicate (TEOS, 98%), and 3-aminopropyltriethoxysilane (APTES, 95%) were purchased from Sigma-Aldrich. Ammonium hydroxide (28.0% – 30.0%), cyclo-hexane (HPLC grade), and ethanol were obtained from Fisher Scientific Co. Carboxytetramethylrhodamine-succinimidyl ester (TAMRA-SE) was purchased from Molecular Probes. Deionized (DI) water (Millipore Milli-Q grade) with resistivity of 18.2 MΩ•cm was used in all experiments.

A Hitachi SU8010 field emission scanning electron microscope (SEM) was used for imaging the composite of silica nanoparticles and graphene oxide. A Hitachi 7500 transmission electron microscope (TEM) was used to take the images and measure the diameters of silica nanoparticles. UV-vis absorption spectra were recorded with a Lambda 1050 UV/VIS/NIR spectrometer. A Jobin Yvon Horiba Fluorolog spectrofluorometer was employed for fluorescence intensity and lifetime measurements. Zeta potential was detected using a Zetasizer (Marlwen, model of Nano-ZS). An Eppendorf 5810 R centrifuge was used to centrifuge silica nanoparticles after washing.

Synthesis of SiNPs@TAMRA. First, silica nanoparticles (SiNPs) were synthesized using the reverse microemulsion method. The Briefly, 7.5 mL of cycle-hexane, 1.6 mL of 1-hexanol, 1.8 mL of triton X-100, and 0.48 mL of H_2O were mixed with vigorous stirring. After stirring for 15 min, 100 μ L of NH4OH was added followed by the addition of 400 μ L of TEOS to initiate the formation of silica nanoparticles. After 30

min of stirring, $80~\mu L$ of APTES was added to co-polymerize with the TEOS for forming amino groups on the surface of SiNPs. The reaction could be carried out overnight and followed up with ethanol and water wash. Finally, the formed SiNPs with amino groups were dispersed in 20.0~mL water with concentration of 4.0~mg/mL. For conjugating TAMRA onto the surface of SiNPs, 20.0~mL of 4.0~mg/mL SiNPs was mixed with 0.5~mL of TAMRA-SE and allowed to conjugate overnight. The SiNPs@TAMRA was then washed with water three times to obtain a 4.0~mg/mL SiNPs@TAMRA aqueous solution.

Formation of SiNPs@TAMRA@Si-NH₂. To coat a layer of silica on the surface of SiNPs@TAMRA with varying thicknesses, the modified Stöber method was used. Briefly, 10.0 mL of EtOH, 0.2 mL of 4.0 mg/mL SiNPs@TAMRA prepared in the previous step, 1.8 mL of water, 0.50 mL of NH₄OH, and different amounts of TEOS, ranging from 0.31.0, 2.0,4.0, and 10.0 μ L, were stirred together for 2 hours. Then 0.15,0.50, 1.00, 2.00, and 7.50 μ L of APTES was added into the mixture to form amino groups on the surface of silica shell. After 0.5 hour of stirring, EtOH and water were used to wash the SiNPs@TAMRA@Si-NH₂ via centrifugation.

Formation of SiNPs@Rubpy@Si-NH₂. First, the SiNP cores were synthesized using the reverse microemulsion method as described in the previous section. Then, a silica coating process coupled with doping Rubpy was carried out by the modified Stöber method. Briefly, 10.0 mL of EtOH, 2.0 mL of 4.0 mg/mL SiNPs prepared in the previous step, 0.50 mL of NH₄OH, 1.0 mL of 0.1 M Rupby solution and 20 μL of TEOS were mixed to start doping of Rubpy into the silica shell. Furthermore, to adjust the distance between the Rubpy and GO, different thicknesses of silica shell were generated by altering the amount of TEOS and APTES using the similar Stöber method.

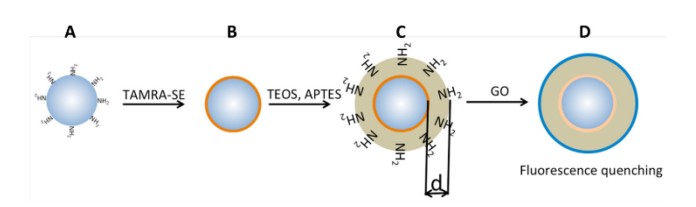
Fluorescence Quenching Measurement. The experiment was carried out using a Jobin Yvon Horiba Fluorolog spectrofluorometer. Briefly, 100 μL of SiNPs@TAMRA@SiNH2 or SiNPs@Rubpy@Si-NH2 (equi 0.1 nM TAMRA or 0.1 nM Rubpy) solution was placed in a quartz cuvette for the fluorescence measurement. For the TAMRA measurements, the excitation wavelength was set at 540 nm, and the fluorescence spectrum was recorded from 560 nm to 650 nm. For the Rubpy measurements, the excitation wavelength was set at 460 nm, and the fluorescence spectrum was recorded from 560 nm to 750 nm. The slits for excitation and emission were set at 5 nm. After recording of the original fluorescence spectrum of nanoparticles, 1 μL of 5 mg/mL GO was added into the solution and mixed using a pipette. The fluorescence spectrum was measured 2 min later to investigate the quenching effect.

Fluorescence Lifetime Measurement. A 100 μ L aliquot of SiNPs@TAMRA@Si-NH₂ (equi 0.1 nM TAMRA) solution was loaded into a quartz cuvette for lifetime measurement. The fluorescence lifetime was collected using a Jobin Yvon Horiba Fluorolog spectrofluorometer equipped with a LED laser. The LED laser light source at 494 nm was used for the excitation. A Ludox SM-30 colloidal silica was used as the reference to measure the lifetime. The emission data was collected at 575 nm with an 8-nm slit. Datastation software was used to collect

the data and then analyzed by Decay Analysis System from Horiba Scientific.

RESULTS AND DISCUSSION

Design of the Nanostructure Model for Studying Fluorescence Quenching Ability of GOs. To investigate the fluorescence quenching ability of GOs, a nanostructure model with a rigid and thickness adjustable spacer is needed. To achieve this goal, we designed a four-layer core-shell nanostructure with a silica shell as a spacer between GOs and fluorophores. The nanostructure can provide accurate distance that would bypass the effect of inaccurate distance calculation with the DNA strand spacer.^{28, 29} Our design was shown in Scheme 1. First, a silica nanoparticle was prepared as a core platform for dye molecules. Silica was chosen because its inert feature that would not affect fluorophore properties. To adhere dye molecules onto the silica core, amino groups were formed on the silica core surface during the synthesis of silica nanoparticles (Scheme 1 A). Thus, a fluorophore, TAMRA-SE, could be conjugated onto the SiNPs through the interaction of amino groups with succinimidyl ester group on TAMRA-SE (Scheme 1 B). At this moment, the dye molecule platform was well prepared for fluorescence quenching studying. To build an effective nanostructure model, the fabrication of a rigid and thickness adjustable spacer is a critical step. A silica shell was selected for this function. The silica shell is rigid, stable, and inert based on our previous studies on fabrication of silica-based nanostructures. 31, 36 The Stöber method was used for forming a layer of silica on the structure. In this coating process, APTES was added for co-polymerization with TEOS to form amino groups on the surface of the final nanoparticles (SiNPs@TAMRA@Si-NH₂). The amino groups provided the positive charges for later adhering of GOs. The thickness (d) of the silica shell could be manipulated by using different amount of TEOS and APTES (Scheme 1 C). Afterwards, the thickness can be accurately measured on the SEM/TEM images of the resultant nanostructure. Finally, negatively charged GOs were adhered to the surface of SiNPs@TAMRA@Si-NH2 through electrostatic interaction (Scheme 1 D). The designed nanostructure could be a model for studying fluorescence quenching ability of GOs.



Scheme 1. Schematic diagram of synthesis of a nanostructure model (SiNPs@TAMRA@Si-NH₂) for studying fluorescence quenching ability of GO. (A). Aminomodified silica nanoparticle; (B). The nanoparticle was conjugated with TAMRA through succinimidyl ester. (C). A rigid silica shell with different thickness was formed to separate the fluorophore and GO. (D). GO wrapped the silica nanocomposite tightly by the strong electrostatic interaction between the second layer of amino-silica and GO.

Characterization of the Nanostructure Model. The synthesis of silica core and doping dye molecules into the nanostructure (Scheme 1A-C) was performed successfully based on our previous experiments. 30-31 The most challenging step in our design is the wrapping of GO onto the silica-dye core-shell structure (Scheme 1D). The morphology and flexibility of GO are two important factors to determine whether or not the GO could be wrapped onto the nanoparticle as designed. Thus, we first characterized the shape and size of the GO using a scanning electron microscope (SEM). The 5 mg/mL GO solution was prepared for SEM imaging by dispersion of solid GO to water with 2 hours of ultrasonication. The SEM (Figure 1 A) and STEM (Figure 1B) images showed that the GO sheet size is in a micrometer range. The wrinkles of GO could be observed clearly from the SEM image, indicating its flexibility. This flexibility along with the large size provide GO with good feasibility of wrapping the silica nanoparticles through electrostatic interaction as designed in Scheme 1D. Afterwards, we have qualitatively characterized the GO using UV-vis absorption spectrometry. As shown in Figure 1C, the strong absorption peak at ca. 230 nm was due to the π -plasmon of the sp^2 carbon structure, and the shoulder around 300 nm was ascribed to the n to π^* transitions. The UV-vis spectrometry results confirmed the presence of GO.

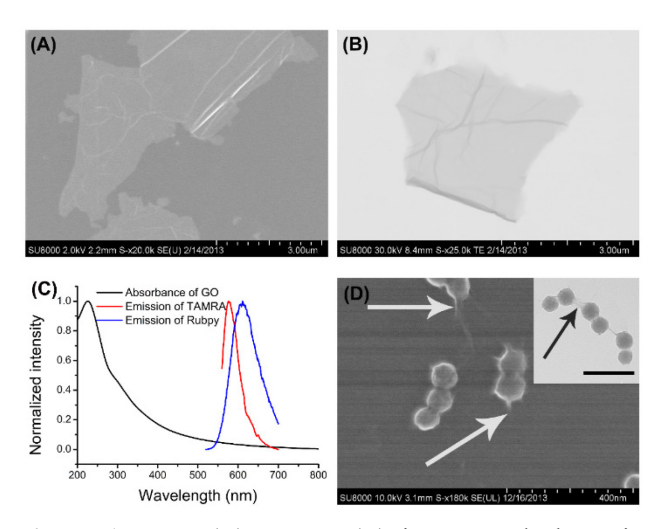


Figure 1. SEM (A), STEM (B) images and absorption spectra (C) of GOs. (D) SEM image of SiNPs@TAMRA with GOs. Inset is a TEM image of SiNPs@TAMRA with GOs, the bar is 200 nm. The white arrows indicate the wrinkle of GO wrapped on the surface of nanoparticles.

We then tested the wrapping ability of GO onto the silicadye core-shell nanoparticles. Due to the electrostatic interaction between the positively charged SiNPs and the negatively charged GO, the GO should be wrapped onto the surface of SiNPs@TAMRA when they were mixed together. Prior to wrapping, the surface charge of the nanostructure (Scheme 1 C) and the GO were confirmed by measuring their Zeta-potential. After the wrapping, the wrapping effect were characterized using TEM and SEM images as shown in Figure 1D. The wrinkles on the edges of SiNPs@TAMRA (white arrow) clearly indicated a total coverage of the GO onto the

SiNPs@TAMRA. The distance between TAMRA and GO was estimated at 0 nm because the TAMRA was covalently conjugated onto the surface of SiNPs and the GO was compactly wrapped on the surface of SiNPs. These results demonstrated the success of fabrication of the designed nanostructure.

Fluorescence Quenching of GO on the SiNPs@TAMRA@Si-NH2 Nanostructure. Fluorescence quenching is a newly discovered property of GO. A fundamental understanding of this quenching ability to various fluorophores is needed. Thus, we initially investigated the quenching ability of GO to a common dye molecule, TAMRA, using our designed nanostructure (Scheme 1). Several important factors, including fluorophore lifetime, GO concentration and spacer distance, were investigated in detail.

The fluorescence quenching ability of GOs was initially tested using the designed nanostructure. Both UV-vis absorption spectrometry and fluorescence emission spectrometry were employed for this test. First, the UV-vis absorption of SiNPs@TAMRA was measured. As shown in Figure 2A curve a, the UV-vis spectrum showed the absorption peak of TAMRA. After wrapping the NPs with GO, the absorbance increased (Figure 2 A curve b) due to the contribution of GO. In a parallel experiment, their fluorescence emission was measured as shown in Figure 2B. The SiNP@TAMRA showed a fluorescence emission peak at 575 nm (Figure 2B curve a). After GO wrapping (Figure 2B curve b), the fluorescence intensity of TAMRA was quenched by ~ 93.4 % based on the comparison of curve a and b in Figure 2B. The result clearly demonstrated the quenching ability of GO to fluorophores.

In order to investigate the mechanism of the fluorescence quenching property of GO, the lifetime of SiNPs@TAMRA before and after GO wrapping was measured. As shown in Figure 2C, curve a is a reference of Ludox SM-30 colloidal silica for the lifetime measurement. Before GO wrapping, the lifetime of SiNPs@TAMRA was 2.12 ± 0.02 ns (Figure 2C, curve b). After the GO wrapping, the fluorescence lifetime of SiNPs@TAMRA decreased to 0.20 ± 0.02 ns (Figure 2D). The quenching efficiency was found to be 90.6% calculated from the lifetime change as below:

$$Q = 1 - \tau/\tau_0 \tag{1}$$

where τ_0 and τ are the lifetime of SiNPs@TAMRA without and with GO wrapping, respectively. The quenching efficiency is comparable with the value calculated using the fluorescence intensity change. Based on the fluorescence quenching theory, the close value of quenching efficiency calculated from the total fluorescence intensity and lifetime measurement indicates that the main quenching mechanism is dynamic quenching. Meanwhile, the similar pattern of their absorption spectra supported this fluorescence quenching mechanism of the GO to fluorophores.

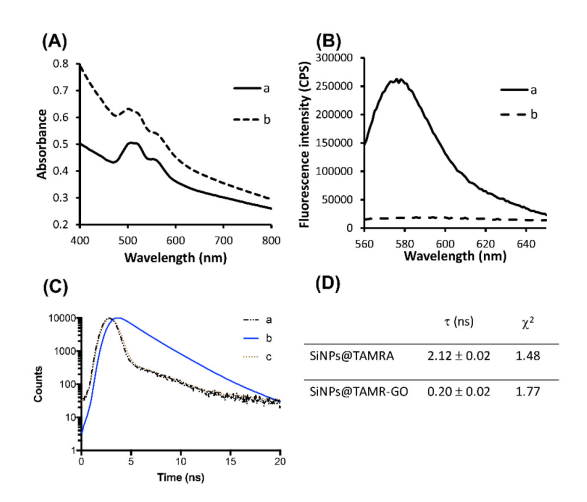


Figure 2. UV-vis absorption (A) and fluorescence emission (B) spectra of SiNPs@TAMRA without (a) and with (b) GOs. λ_{ex} = 540 nm. (C) Lifetime measurement. Curve a is the reference of Ludox SM-30 colloidal silica. b. SiNPs@TAMRA before GO wrapping. c. SiNPs@TAMRA after GO wrapping. A 492 nm LED laser was used in the lifetime measurement.

The concentration of GO will play an important role in the quenching efficiency. In order to find the maximum quenching efficiency of GO to SiNPs@TAMRA, we measured fluorescence intensities of SiNPs@TAMRA with different concentration of GOs at a constant concentration of SiNPs@TAMRA. As shown in Figure 3A, the fluorescence emission intensity of SiNPs@TAMRA decreased significantly with the increase of GO concentration from 1.0 to 10.0 μg/mL. Based on emission peak value at 575 nm in Figure 3A, the fluorescence quenching efficiencies were calculated and plotted vs the GO concentration (Figure 3 B). Figure 3B clearly showed that the quenching efficiency reached a plateau when 10 µg/mL of GO was used. The quenching constant was calculated as 1.431 as shown in inset of Figure 3B. Further increasing the concentration of GO, the fluorescence quenching efficiency remained constant. In the following experiments, to exclude the GO concentration influence, an excess amount of 50 µg/mL GO was used.

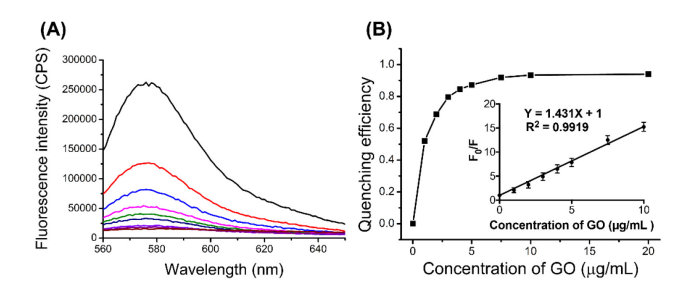


Figure 3. Fluorescence quenching of SiNPs@TAMRA with different concentration of GOs. (A) Fluorescence spectra of SiNPs@TAMRA with different concentrations of GO. From top to bottom: 0, 1.0, 2.0, 3.0, 4.0, 5.0, 7.5, 10.0 and 20.0

 μ g/mL of GOs. (B) Quenching efficiency of GOs to SiNPs@TAMRA with varying concentration of GOs. $\lambda_{ex} = 540$ nm; $\lambda_{em} = 575$ nm.

In FRET theory, the distance between the quencher and the fluorophore is a determining factor for the quenching effect. Therefore, the distance between TAMRA and GO was adjusted by manipulating silica shell thickness. The thickness was determined by the amount of TEOS and APTES used in the synthetic process using the Stöber method. As shown in Figure 4, a few different thicknesses of silica shell were obtained. The exact distance between TAMRA and GO was measured by measuring both radius of SiNPs@TAMRA (Figure 4A) and SiNPs@TAMRA@Si-NH₂ (Figure 4 B-F), then the radius of SiNPs@TAMRA was subtracted from the SiNPs@TAMRA@Si-NH2. Form Figure 4B to 4F, with the increase in the amount of TEOS, the spacer thickness was obtained as 0.3, 1.2, 6.5, 14.7, and 34.5 nm. The thickness of the silica spacer had a linear relationship with the amount of TEOS added into the reaction (Figure 4G). Meanwhile, the amino group on the surface of the silica nanoparticles provided the positive charge for later attachment of GOs.

Figure 4. TEM images of SiNPs@TAMRA@Si-NH₂ with different thicknesses of silica spacer. A. Silica core. B to F: the thicknesses of the spacer were 0.3, 1.2, 6.5, 14.7, and 34.5 nm. (G) The relationship between the amount of TEOS and the thickness of the silica spacer. Y is the thickness of the spacer, X is the amount of TEOS added into the reaction with the unit of mg.

The fluorescence quenching efficiency was then studied using the obtained nanostructure with varying length of the spacers. A solution of 50 µg/mL GO was introduced to the concentration of SiNPs@TAMRA@Si-NH₂ nanostructure solution and their fluorescence emission spectra (Figure 5A) were measured. The results clearly demonstrated that the fluorescence intensity of TAMRA was quenched at different extent. Thickness of the silica shell appeared to be inversely correlated with the quenching effect (Figure 5 A curve a to f). The quenching efficiency was then calculated based on the data in Figure 5 A, and the results were shown in Figure 5B. Interestingly, when the distance between TAMRA and GO was larger than 30 nm, the quenching efficiency of GO was still around 30 %, which indicated the long-distance quenching ability of GO. Theoretically, in contrast to the traditional FRET process with d⁻⁶ dependency,²⁷ the energy transfer rate from a fluorophore to GO should follow d-4 dependency, which implied that GO would quench fluorescence in the range of 30 nm.²⁶ Our results confirmed the theory by showing stronger quenching ability of GOs than a traditional fluorescence quencher.

According to theoretical calculations, the quenching efficiency (Q) of GO with respect to distance is:

$$Q = 1/[1 + (\frac{d}{d0})^4] \tag{2}$$

where d is the distance between graphene and fluorophore, and d_0 is the variable characteristic distance. d_0 is found to be slightly different in various systems, ranging from ~ 5 to 8 nm. $^{28,\ 37}$ By measuring the quenching efficiency of our TAMRA-GO system, GO quenched $\sim 50\%$ of TAMRA fluorescence when the thickness of the silica spacer was ~ 6.54 nm (Figure 5B), which indicates that d_0 is 6.54 nm in the TAMRA-GO system. The quenching efficiency calculated from the steady-state fluorescence reflected total quenching, including both static and dynamic components.

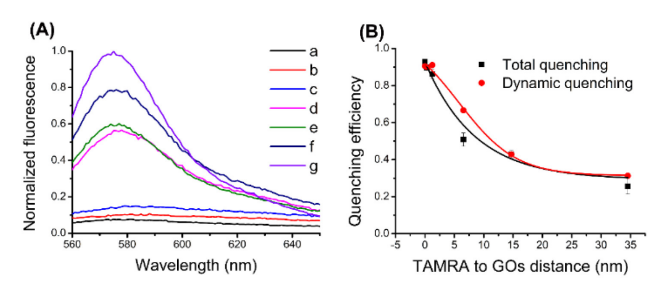


Figure 5. (A) Fluorescence spectra of SiNPs@TAMRA@SiNH₂ with GO. The distances between TAMRA and GO were 0, 0.3, 1.2, 6.5, 14.7, 34.5 nm (curve a to f). Curve g was SiNPs@TAMRA without addition of GO. (B) Quenching efficiency of the doped TAMRA as a function of the spacer length. The quenching efficiency was calculated based on average fluorescence lifetime (squares) and from steady-state fluorescence intensity (circles). The concentration of

nanoparticles was equal ca 0.1 nM of TAMRA. λ_{ex} = 540 nm; λ_{em} = 575 nm.

We then measured the lifetime of TAMRA when GO was present to quench the fluorescence. The quenching efficiency was calculated by $Q=1-\tau/\tau_0$, where τ_0 is the lifetime of TAMRA in the absence of GO, and τ is the lifetime of TAMRA in the presence of GO. As shown in Figure 5B, the quenching efficiency calculated from lifetime was plotted against the thickness of silica shell. As expected, the quenching efficiency was decreased with the increase of the thickness of silica shell. The two methods showed a similar quenching efficiency, indicating that the main quenching mechanism was dynamic quenching.

Fluorescence Quenching GO SiNPs@Rubpy@Si-NH2. In order to understand whether or not GO is a universal fluorophore quencher, we tested an additional dye molecule, Tris(bipyridine)ruthenium(II) chloride (Rubpy), which is another commonly used fluorescent dye molecule with an emission of 600 nm. Instead of the covalent conjugation between amino groups on silica nanoparticles and TAMRA, the Rubpy was doped into a thin layer of silica shell (SiNPs@Rubpy). Then, another layer of pure silica shell spacer was coated on the surface of Rubpy-doped silica nanoparticles and followed with the modification of amino groups (SiNPs@Rubpy@Si-NH₂). The distance between Rubpy and GO was calculated by subtracting the radius of SiNPs@Rubpy from the radius of SiNPs@Rubpy@Si-NH₂. The distances of 2.4, 3.0, 3.7, 4.8, 7.8, 10.1 and 15.6 nm were obtained (Figure 6).

We first investigated the quenching efficiency of GOs to SiNPs@Rubpy with different concentrations of GOs (Figure 7). As the concentration of GO increased, the fluorescence intensity of Rubpy at 600 nm decreased and quenching efficiency reached a pleatou when the concentration of GO was 50 μg/mL. Therefore, we chose 50 μg/mL of GO for the following quenching efficiency investigation. The quenching constant was calculated as 0.1332 as shown in inset of Figure 7B. As shown in Figure 8A, by increasing the distance between Rubpy and GO, the fluorescence intensity of Rubpy recovered from the quenching state. The quenching efficiency calculated from the steady-state fluorescence intensity was plotted against the distance (Figure 8B). The characteristic distance was evaluated to be around 5.0 nm, which was smaller than that of the TAMRA when the quenching efficiency was 50 %. The lifetime of Rubpy was dramatically decreased when it was doped into the thin layer of silica shell, which was out of the detection limit of our instrument. Therefore, the dynamic quenching mode was not investigated. Overall, GO can also quench the fluorescence of Rubpy with a distance-dependent manner in a long range.

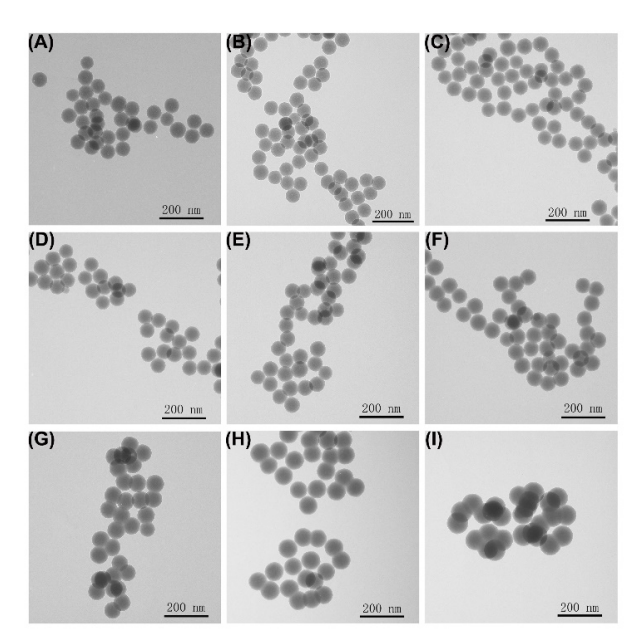


Figure 6. TEM images of SiNPs (A), SiNPs@Rubpy (B), and SiNPs@Rubpy@Si-NH₂ with different spacer thicknesses of 2.4, 3.0, 3.7, 4.8, 7.8, 10.1, and 15.6 nm (C to I).

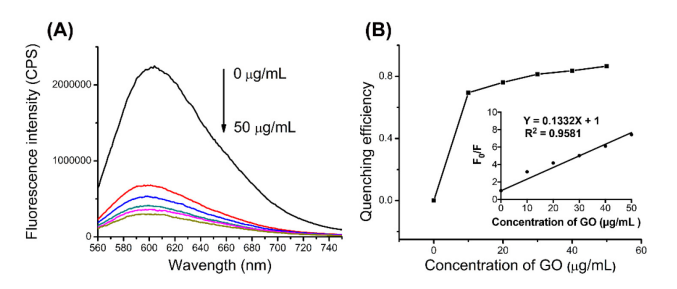


Figure 7. Fluorescence quenching of SiNPs@Rubpy with different concentrations of GOs. (A) Fluorescence spectra of SiNPs@ RuBpy with different concentrations of GOs. From top to bottom: 0, 10, 20, 30, 40 and 50 μ g/mL. (B) Quenching efficiency GOs to SiNPs@ RuBpy with different concentrations. $\lambda_{ex} = 460$ nm; $\lambda_{em} = 600$ nm.

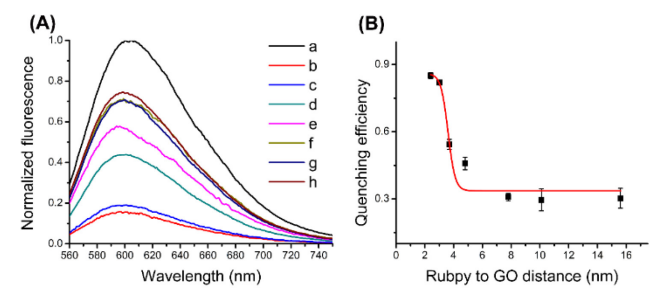
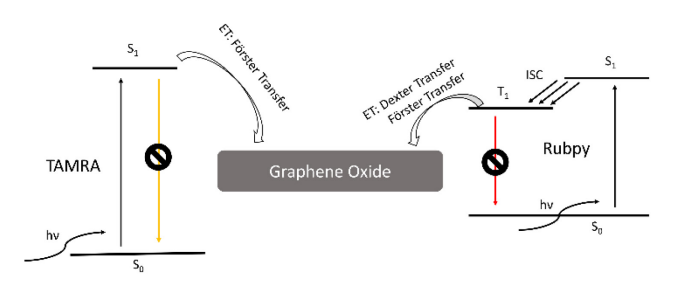


Figure 8. (A) Fluorescence spectra of SiNPs@Rubpy (a) and SiNPs@Rubpy@Si-NH₂ with 50 μg/mL GO. The distances between Rubpy and GO were separated by 2.4, 3.0, 3.7, 4.8, 7.8, 10.1, and 15.6 nm silica spacer (curve b to h). (B) Quenching efficiency of the doped Rubpy as a function of the distance. The concentrations of nanoparticles were equal ca 0.1 nM of Rubpy. $λ_{ex}$ = 460 nm; $λ_{em}$ = 600 nm.

Mechanisms for Fluorescence Quenching of GOs. As shown in Figure 5B and Figure 8B, the GOs have different quenching behaviors for the two different dyes. Based on these results, we proposed quenching mechanism as shown in Scheme 2. The organic fluorophore TAMRA was mainly quenched by Förster resonance energy transfer (FRET), which has been illustrated in a number of publications. 28-29, 38 Therefore, the TAMRA-GO system showed a typical FRETbased distance-dependent quenching curve (Figure 5B). In contrast, Rubpy is an organometallic dye, which emits longlifetime (~600 nm) phosphorescence through the excited triplet state.³⁹ However, the energy level of the excited triplet state of Rubpy (-3.934 eV)⁴⁰ was closely followed by the potential of GO conduction band (-4.70 eV)⁴¹. Therefore, the quenching process by GO was a preferred pathway instead of the phosphorescence emission. In the Rubpy quenching process by GOs, two different energy transfer mechanisms may be involved, including the direct exchange of electrons (Dexter transfer) and the coupling of transition dipoles (Förster transfer). The exchange of electrons (Dexter transfer) could only be efficient in a very short donor-acceptor distance with an interpenetration of their orbitals.⁴² In our model, the Rubpy was fixed in the silica shell, which restricted the molecular diffusion and collision with GOs. Therefore, in the system of Rubpy and GO, Dexter transfer might be the main mechanism only when the distance was very short, demonstrating a sharp decrease of quenching efficiency with the distance increase (Figure 8B). When the distance increased again, the main mechanism of quenching became the Förster transfer, which could be efficient even larger than 10 nm in the case of GO as the acceptor.



Scheme 2. Proposal to the different quenching behavior of GO to TAMRA and Rubpy. The TAMRA was quenched through the Förster transfer from the excited singlet state. In contrast, Rubpy was quenched through both Förster transfer and Dexter transfer from the excited triplet state.

CONCLUSIONS

In conclusion, we have demonstrated the quenching ability of GOs to two different fluorophores including TAMRA and Rubpy. The distance between the fluorophore and GOs was adjusted by a layer of rigid silica spacer, which is more consistent and accurate in thickness than the soft DNA strands. The quenching efficiency of GO to these two fluorophores followed a distance-dependent manner with characteristic distance of 6.54 and 5.0 nm, respectively. By comparing the steady-state total quenching efficiency and dynamic quenching efficiency of GO to TAMRA, we found that the main quenching mechanism was dynamic quenching - energy transfer. Moreover, the quenching range of GO to these fluorophores

was much greater than the traditional FRET distance (10 nm). By exploring the long-range quenching properties of GOs to fluorophores, the applications of GO could be expanded to a broader range.

AUTHOR INFORMATION

Corresponding Author

*To whom correspondence should be addressed: Phone: 701-777-3610. Fax: 701-777-2331. E-mail: julia.zhao@und.edu.

ACKNOWLEDGMENT

This work was supported by the USA National Science Foundation Grants CHE 1709160, University of North Dakota Postdoctoral Pilot Program supported by UND VPR and Art and Science College, Applied Research to Address the State's Critical Needs Initiative grant supported by College of Arts & Sciences of UND, and the North Dakota Industrial Commission Grant G-041-081.

REFERENCES

- 1. Yang, K.; Li, Y.; Tan, X.; Peng, R.; Liu, Z. Behavior and Toxicity of Graphene and Its Functionalized Derivatives in Biological Systems. *Small* **2013**, *9*, 1492-1503.
- 2. Novoselov, K. S.; Falko, V. I.; Colombo, L.; Gellert, P. R.; Schwab, M. G.; Kim, K. A Roadmap for Graphene. *Nature* **2012**, *490*, 192-200.
- 3. Lightcap, I. V.; Kamat, P. V. Graphitic Design: Prospects of Graphene-Based Nanocomposites for Solar Energy Conversion, Storage, and Sensing. *Acc. Chem. Res.* **2012**, *46*, 2235-2243.
- 4. Chen, D.; Feng, H.; Li, J. Graphene Oxide: Preparation, Functionalization, and Electrochemical Applications. *Chem. Rev.* **2012**, *112*, 6027-6053.
- 5. Eda, G.; Lin, Y.-Y.; Mattevi, C.; Yamaguchi, H.; Chen, H.-A.; Chen, I. S.; Chen, C.-W.; Chhowalla, M. Blue Photoluminescence from Chemically Derived Graphene Oxide. *Adv. Mater.* **2010**, 22, 505-509.
- 6. Chien, C. T.; Li, S. S.; Lai, W. J.; Yeh, Y. C.; Chen, H. A.; Chen, I. S.; Chen, L. C.; Chen, K. H.; Nemoto, T.; Isoda,

- S.; Chen, M.; Fujita, T.; Eda, G.; Yamaguchi, H.; Chhowalla, M.; Chen, C. W. Tunable Photoluminescence from Graphene Oxide. *Angew. Chem. Int. Ed.* **2012**, 51, 6662-6666.
- 7. Luo, Z.; Vora, P. M.; Mele, E. J.; Johnson, A. T. C.; Kikkawa, J. M. Photoluminescence and Band Gap Modulation in Graphene Oxide. *Appl. Phys. Lett..* **2009**, 94, 111909-111903.
- 8. Dreyer, D. R.; Park, S.; Bielawski, C. W.; Ruoff, R. S. The Chemistry of Graphene Oxide. *Chem. Soc. Rev.* **2010**, 39, 228-240.
- 9. Ramakrishna Matte, H. S. S.; Subrahmanyam, K. S.; Venkata Rao, K.; George, S. J.; Rao, C. N. R. Quenching of Fluorescence of Aromatic Molecules by Graphene Due to Electron Transfer. *Chem. Phys. Lett..* **2011**, 506, 260-264.
- 10. Liu, Y.; Liu, C.-y.; Liu, Y. Investigation on Fluorescence Quenching of Dyes by Graphite Oxide and Graphene. *Appl. Surf. Sci.* **2011**, 257, 5513-5518.
- 11. Dong, H.; Gao, W.; Yan, F.; Ji, H.; Ju, H. Fluorescence Resonance Energy Transfer between Quantum Dots and Graphene Oxide for Sensing Biomolecules. *Anal. Chem.* **2010**, 82, 5511-5517.
- 12. Dong, H.; Zhang, J.; Ju, H.; Lu, H.; Wang, S.; Jin, S.; Hao, K.; Du, H.; Zhang, X. Highly Sensitive Multiple microRNA Detection Based on Fluorescence Quenching of Graphene Oxide and Isothermal Strand-Displacement Polymerase Reaction. *Anal. Chem.* **2012**, 84, 4587-4593.
- 13. Huang, P. J.; Liu, J. Molecular Beacon Lighting up on Graphene Oxide. *Anal. Chem.* **2012**, 84, 4192-4198.
- 14. Thangaraj, V.; Bussiere, J.; Janot, J.-M.; Bechelany, M.; Jaber, M.; Subramanian, S.; Miele, P.; Balme, S. Fluorescence Quenching of Sulfo-rhodamine Dye over Graphene Oxide and Boron Nitride Nanosheets. *Eur. J. Inorg. Chem.* **2016**, *2016*, *2125-2130*.
- 15. Chung, C.; Kim, Y.-K.; Shin, D.; Ryoo, S.-R.; Hong, B. H.; Min, D.-H. Biomedical Applications of Graphene and Graphene Oxide. *Acc. Chem. Res.* **2013**, *46*, 2211-2224.
- 16. Liu, Y.; Dong, X.; Chen, P. Biological and Chemical Sensors based on Graphene Materials. *Chem Soc Rev* **2012**, *41*, 2283-2307.
- 17. Sreejith, S.; Ma, X.; Zhao, Y. Graphene Oxide Wrapping on Squaraine-Loaded Mesoporous Silica Nanoparticles for Bioimaging. *J. Am. Chem. Soc.* **2012**, *134*, 17346-17349.
- 18. He, S.; Song, B.; Li, D.; Zhu, C.; Qi, W.; Wen, Y.; Wang, L.; Song, S.; Fang, H.; Fan, C. A Graphene Nanoprobe for Rapid, Sensitive, and Multicolor Fluorescent DNA Analysis. *Adv. Funct. Mater.* **2010**, 20, 453-459.

- 19. Li, F.; Pei, H.; Wang, L.; Lu, J.; Gao, J.; Jiang, B.; Zhao, X.; Fan, C. Nanomaterial-Based Fluorescent DNA Analysis: A Comparative Study of the Quenching Effects of Graphene Oxide, Carbon Nanotubes, and Gold Nanoparticles. *Adv. Funct. Mater.* **2013**, 23, 4140-4148.
- 20. Tu, Y.; Li, W.; Wu, P.; Zhang, H.; Cai, C. Fluorescence Quenching of Graphene Oxide Integrating with the Site-Specific Cleavage of the Endonuclease for Sensitive and Selective MicroRNA Detection. *Anal. Chem.* **2013**, 85, 2536-2542.
- 21. Jang, H.; Ryoo, S.-R.; Kim, Y.-K.; Yoon, S.; Kim, H.; Han, S. W.; Choi, B.-S.; Kim, D.-E.; Min, D.-H. Discovery of Hepatitis C Virus NS3 Helicase Inhibitors by a Multiplexed, High-Throughput Helicase Activity Assay Based on Graphene Oxide. *Angew. Chem. Int. Ed.* **2013**, 52, 2340-2344.
- 22. Jang, H.; Kim, Y. K.; Kwon, H. M.; Yeo, W. S.; Kim, D. E.; Min, D. H. A Graphene-Based Platform for the Assay of Duplex-DNA Unwinding by Helicase. *Angew. Chem. Int. Ed.* **2010**, 49, 5703-5707.
- 23. Lu, C. H.; Yang, H. H.; Zhu, C. L.; Chen, X.; Chen, G. N. A Graphene Platform for Sensing Biomolecules. *Angew. Chem. Int. Ed.* **2009**, 48, 4785-4787.
- 24. Zhang, C.; Yuan, Y.; Zhang, S.; Wang, Y.; Liu, Z. Biosensing Platform Based on Fluorescence Resonance Energy Transfer from Upconverting Nanocrystals to Graphene Oxide. *Angew. Chem. Int. Ed.* **2011**, 50, 6851-6854.
- 25. Zhang, M.; Yin, B. C.; Tan, W.; Ye, B. C. Versatile Graphene-Based Fluorescence "on/Off" Switch for Multiplex Detection of Various Targets. *Biosens. Bioelectron.* **2011**, 26, 3260-3265.
- 26. Swathi, R. S.; Sebastian, K. L. Long Range Resonance Energy Transfer from a Dye Molecule to Graphene Has (Distance)[Sup -4] Dependence. *J. Chem. Phys.* **2009**, 130, 086101.
- 27. Schaufele, F.; Demarco, I.; Day, R. N. FRET Imaging in the Wide-Field Microscope. In *Molecular Imaging*, Periasamy, A.; Day, R. N., Eds. American Physiological Society: San Diego, **2005**; 72-94.
- 28. Huang, P.-J. J.; Liu, J. DNA-Length-Dependent Fluorescence Signaling on Graphene Oxide Surface. *Small* **2012**, *8*, 977-983.
- 29. Piao, Y.; Liu, F.; Seo, T. S. The Photoluminescent Graphene Oxide Serves as an Acceptor Rather Than a Donor in the Fluorescence Resonance Energy Transfer Pair of Cy3.5-Graphene Oxide. *Chem. Commun.* **2011**, 47, 12149-12151.
- 30. Xu, S.; Hartvickson, S.; Zhao, J. X. Engineering of SiO2-Au-SiO2 Sandwich Nanoaggregates Using a Building

- Block: Single, Double, and Triple Cores for Enhancement of Near Infrared Fluorescence. *Langmuir.* **2008**, 24, 7492-7499.
- 31. Chen, J.; Jin, Y.; Fahruddin, N.; Zhao, J. X. Development of Gold Nanoparticle-Enhanced Fluorescent Nanocomposites. *Langmuir.* **2013**, 29, 1584-1591.
- 32. Feng, A. L.; You, M. L.; Tian, L.; Singamaneni, S.; Liu, M.; Duan, Z.; Lu, T. J.; Xu, F.; Lin, M. Distance-Dependent Plasmon-Enhanced Fluorescence of Upconversion Nanoparticles using Polyelectrolyte Multilayers as Tunable Spacers. *Sci. Rep.* **2015**, *5*, 7779.
- 33. Feng, A. L.; Lin, M.; Tian, L.; Zhu, H. Y.; Guo, H.; Singamaneni, S.; Duan, Z.; Lu, T. J.; Xu, F. Selective Enhancement of Red Emission from Upconversion Nanoparticles via Surface Plasmon-Coupled Emission. *RSC Adv.* **2015**, *5*, 76825-76835.
- 34. Luo, Q.; Chen, Y.; Li, Z.; Zhu, F.; Chen, X.; Sun, Z.; Wei, Y.; Guo, H.; Wang, Z. B.; Huang, S. Large Enhancements of NaYF4:Yb/Er/Gd Nanorod Upconversion Emissions via Coupling with Localized Surface Plasmon of Au Film. *Nanotechnology* **2014**, *25*, 185401.
- 35. Yuan, H.; Khatua, S.; Zijlstra, P.; Yorulmaz, M.; Orrit, M. Thousand-Fold Enhancement of Single-Molecule Fluorescence Near a Single Gold Nanorod. *Angew. Chem. Int. Ed.* **2013**, *52*, 1217-1221.
- 36. Yi, Z.; Liu, M.; Luo, J.; Zhao, Y.; Zhang, W.; Yi, Y.; Yi, Y.; Duan, T.; Wang, C.; Tang, Y. Multiple surface plasmon resonances of square lattice nanohole arrays in Au-SiO2-Au multilayer films. *Opt. Commun.* **2017**, *390*, 1-6.
- 37. Wang, Y.; Kurunthu, D.; Scott, G. W.; Bardeen, C. J. Fluorescence Quenching in Conjugated Polymers Blended with

- Reduced Graphitic Oxide. J. Phys. Chem. C. 2010, 114, 4153-4159
- 38. de Miguel, M.; Alvaro, M.; Garcia, H. Graphene as a Quencher of Electronic Excited States of Photochemical Probes. *Langmuir* **2012**, *28*, 2849-2857.
- 39. Mori, K.; Kawashima, M.; Che, M.; Yamashita, H. Enhancement of the Photoinduced Oxidation Activity of a Ruthenium(II) Complex Anchored on Silica-Coated Silver Nanoparticles by Localized Surface Plasmon Resonance. *Angew. Chem. Int. Ed.* **2010**, *49*, 8598-8601.
- 40. Inglez, S. D.; Lima, F. C. A.; Camilo, M. R.; Daniel, J. F. S.; Santos, E. D. A.; Lima-Neto, B. S.; Carlos, R. M. Tuning of Photochemical and Photophysical Properties of [RuII(2,2'-bipyridine)2Lx] Complexes Using Nonchromophoric Ligand Variations. *J. Braz. Chem. Soc.* 2010, 21, 157-168.
- 41. Zhao, Y.; Li, K.; He, Z.; Zhang, Y.; Zhao, Y.; Zhang, H.; Miao, Z. Investigation on Fluorescence Quenching Mechanism of Perylene Diimide Dyes by Graphene Oxide. *Molecules* **2016**, *21*, 1642.
- 42. Murphy, C. B.; Zhang, Y.; Troxler, T.; Ferry, V.; Martin, J. J.; Jones, W. E. Probing Förster and Dexter Energy-Transfer Mechanisms in Fluorescent Conjugated Polymer Chemosensors. *J. Phys. Chem. B.* **2004**, *108*, 1537-1543.

Insert Table of Contents artwork here

